*June 2009* *Volume 5 Issue 3*

Trade Science Inc.

Materials Science

An Indian Journal

Full Paper

MSAIJ, 5(3), 2009 [175-183]

# Effect of different filler materials on the abrasive wear behavior of glass fiber reinforced polymer matrix composites

**Amar Patnaik[1]*, Alok Satapathy[2], Sandhyarani Biswas[2]**
**[1]Mechanical Engineering Department, N.I.T.Hamirpur-177005, (INDIA)**
**[2]Mechanical Engineering Department, N.I.T.Rourkela-769008, (INDIA)**
**E-mail : amar_mech@sify.com**
*Received: 3rd May, 2009 ; Accepted: 8th May, 2009*

## ABSTRACT

The incorporation of silicon carbide (SiC), Alumina ($Al_2O_3$) and pine bark dust (PBD) fillers on three-body abrasive wear behaviour of random glass fiber-epoxy resin (RGF-Epoxy) composites has been investigated. Dry sand/ rubber wheel abrasion tests were carried out at 200rpm test speed. The tests were carried out at 50N and 75N loads by varying the abrading distance from 200 to 600m. The mass loss and specific wear rate of the composites reduces significantly on the addition of SiC filler. The predominant wear mechanisms in the case of $Al_2O_3$ composite were plastic deformation, micro-cutting, pitting in the matrix, and fibre removal. In the case of SiC composite the wear mechanisms were micro-cutting, ploughing, fragmentation of wear debris in the matrix and excessive deterioration of fibre surface followed by delamination, while in pine bark dusts the wear mechanisms were micro-cutting in the resin matrix and tearing the fibre transversely at their ends.


## KEYWORDS

Glass fiber;
Epoxy resin;
Abrasive wear;
Pine bark dust;
$Al_2O_3$;
SiC.

## 1. INTRODUCTION

Polymer matrix composites are being increasingly used in industry because of their unique combination of mechanical, electrical, and thermal properties. Typically they have high specific strength and modulus, excellent fracture toughness and fatigue properties, and good corrosion, thermal and electrical resistance properties. This combination of properties, particularly their high strength/ stiffness to weight ratio, make them very attractive materials for transport applications where there is commercial advantage in minimizing vehicle weight. One such application is in the transport and handling of bulk solids. However, their use in this application is limited by an incomplete understanding of their abrasion wear resistance and the means by which this can be controlled and improved. Abrasive wear is caused due to hard particles or hard protuberances that are forced against and move along a solid surface. The abrasive wear process is traditionally divided into two groups: two-body and three-body abrasive wear. In two-body abrasion, wear is caused either by hard protuberances on one surface which can only slide over the other or by the rolling and sliding of hard free-particles on solid surfaces, the former is named as two-body fixed abrasive wear and the latter two-body free-abrasive wear. In three-body abrasion, particles are trapped between two solid surfaces but are free to roll as well as slide.

The rate of material removal in three-body abrasion is one order of magnitude lower than that for two-body fixed-abrasive wear[1], because in three-body abrasion the loose abrasive particles abrade the solid surfaces between which they are situated only about 10% of the time in sliding, while they spend about 90% of time in rolling[2].

Also in the literature, two-body and three body abrasion is usually discussed separately. Engineering polymers and polymer based composites are widely used in design. Polymers and their composites are often required to move in contact with hard abrasive. In recent years research has been devoted to exploring the potential advantage of a thermoplastic matrix for composite materials. One such matrix is olyaryletherke tone (PAEK), which shows exceptional properties due to its semicrystalline character and molecular rigidity of its repeating units. Its high strength and modulus, better toughness, thermal stability, easy processing, chemical inertness, wear and radiation resistance, make it an ideal material for advanced composites. A large amount of data on abrasive wear behaviour of PEEK and their composites reinforced with fibres and fillers have been reported[3-9]. Cirino et al.[3,4] reported the sliding as well as the abrasive wear behaviour of continuous glass, carbon and aramid fibre reinforced PEEK. Lhymn et al.[5] investigated the abrasive wear of short carbon fibre (CF) reinforced PEEK. Voss and Friedrich[6] studied the sliding and abrasive wear behaviour of short glass and CF reinforced PEEK composites at room temperature. Briscoe et al.[7] reported abrasive wear behaviour of PEEK filled PTFE and PTFE filled PEEK. Incorporation of PEEK in PTFE reduced wear rate of PTFE while wear rate increased in the latter case. Harsha and Tewari[8,9] investigated two-body abrasive wear behaviour of various short fibres reinforced PAEK composites. The above investigations were concentrated on two-body abrasion studies of PAEKs and their composites against abrasive papers. According to the author's knowledge, no study is available in the literature on three-body abrasive wear behaviour of pine bark dust reinforced epoxy glass fiber matrix composites.

This paper reports a study of the wear performance of four different composites with and without filler content during abrasion by hard solids particles. The bulk solid abrasives were applied to the surface of the test surfaces under conditions common in industry in which there was limited constraint of the transport of the bulk solid particles. As such, three-body wear was possible, depending on the abrasive/surface interaction. The purpose of this study was to shed light on the transition between the effects of the filler content and the wear media on the wear mechanisms involved were investigated through scanning electron microscopy (SEM) and weight loss measurements.

## 2. EXPERIMENTAL

### 2.1. Specimen preparation

E-glass fibers (360 roving taken from Saint Govion) are reinforced with Epoxy LY 556 resin, chemically belonging to the 'epoxide' family is used as the matrix material. Its common name is Bisphenol A Diglycidyl Ether. The low temperature curing epoxy resin (Araldite LY 556) and corresponding hardener (HY951) are mixed in a ratio of 10:1 by weight as recommended. The epoxy resin and the hardener are supplied by Ciba Geigy India Ltd. E-glass fiber and epoxy resin has modulus of 72.5 GPa and 3.42GPa respectively and possess density of 2590 kg/m$^3$ and 1100kg/m$^3$ respectively. Composites of four different compositions such as 0wt% filler, 10wt% $Al_2O_3$, 10wt% SiC and 10wt% pine bark dust are made and the fiber loading (weight fraction of glass fiber in the composite) is kept at 50% for all the samples. The castings are put under load for about 24 hours for proper curing at room temperature. Specimens of suitable dimension are cut using a diamond cutter for physical characterization and erosion test.

### 2.2. Density

The theoretical density of composite materials in terms of weight fraction can easily be obtained as for the following equations given by Agarwal and Broutman[10].

$$\rho_{ct} = \frac{1}{(W_f/\rho_f)+(W_m/\rho_m)} \quad (1)$$

Where, W and ρ represent the weight fraction and density respectively. The suffix f, m and ct stand for the fiber, matrix and the composite materials respectively. The composites under this investigation consists of three components namely matrix, fiber

and particulate filler. Hence the modified form of the expression for the density of the composite can be written as

$$\rho_{ct} = \frac{1}{(W_f/\rho_f)+(W_m/\rho_m)+(W_p/\rho_p)} \quad (2)$$

Where, the suffix 'p' indicates the particulate filler materials. The actual density ($P_{ce}$) of the composite, however, can be determined experimentally by simple water immersion technique. The volume fraction of voids ($V_v$) in the composites is calculated using the following equation:

$$V_v = \frac{\rho_{ct} - \rho_{ce}}{\rho_{ct}} \quad (3)$$

## 2.3. Tensile strength

The tension test is generally performed on flat specimens. The most commonly used specimen geometries are the dog-bone specimen and straight-sided specimen with end tabs. A uni-axial load is applied through the ends. The ASTM standard test recommends that the specimens with fibers parallel to the loading direction should be 11.5 mm wide. Length of the test section should be 100 mm. The test-piece used here was of dog-bone type and having dimensions according to the standards. The tension test was performed on all the three samples as per ASTM D3039-76 test standards.

## 2.4. Flexural strength

The determination of flexural strength is an important characterization of any structural material. It is the ability of a material to withstand the bending before reaching the breaking point. Conventionally a three point bend test is conducted for finding out this material property. In the present investigation also the composites were subjected to this test in a testing machine Instron 1195. A span of 30 mm was taken and cross head speed was maintained at 10 mm/min. The strength of a material in bending is expressed as the stress on the outermost fibers of a bent test specimen, at the instant of failure. In a conventional test, flexural strength expressed in MPa is equal to

**Flexural Strength = $3PL / 2bd^2$**

Where P= applied central load (N), L= test span of the sample (m), b= width of the specimen (m), d= thickness of specimen under test (m)

## 2.5. Micro-hardness

Micro-hardness measurement is done using a Leitz micro-hardness tester. A diamond indenter, in the form of a right pyramid with a square base and an angle $136^0$ between opposite faces, is forced into the material under a load F. The two diagonals X and Y of the indentation left on the surface of the material after removal of the load are measured and their arithmetic mean L is calculated. In the present study, the load considered F = 24.54N and Vickers hardness number is calculated using the following equation.

$$H_V = 0.1889\frac{F}{L^2} \quad (4)$$

and L = (X+Y) / 2

Where F is the applied load (N), L is the diagonal of square impression (mm), X is the horizontal length (mm) and Y is the vertical length (mm).

## 2.6. Impact strength

Low velocity instrumented impact tests are carried out on composite specimens. The tests are done as per ASTM D 256 using an impact tester. The pendulum impact testing machine ascertains the notch impact strength of the material by shattering the V-notched specimen with a pendulum hammer, measuring the spent energy, and relating it to the cross section of the specimen. The standard specimen for ASTM D 256 is 64 $\times 12.7 \times 3.2$ mm and the depth under the notch is 5.2 mm.

## 2.7. Scanning electron microscopy

The surfaces of the raw fish scales and the composite specimens are examined directly by scanning electron microscope JEOL JSM-6480LV. The scales are washed, cleaned thoroughly, air-dried and are coated with 100 Å thick platinum in JEOL sputter ion coater and observed SEM at 20 kV. Similarly the composite samples are mounted on stubs with silver paste. To enhance the conductivity of the samples, a thin film of platinum is vacuum-evaporated onto them before the photomicrographs are taken.

## 2.8. Abrasive wear test

The schematic representation of rubber wheel test set up is shown in figure 1. In the present study, silica sand (density 2.6 g/cm3) was used as the abrasive. The abrasive particles of AFS 60 grade silica sand were angular in shape with sharp edges.

The shape of the silica sand used for abrasive wear

Full Paper

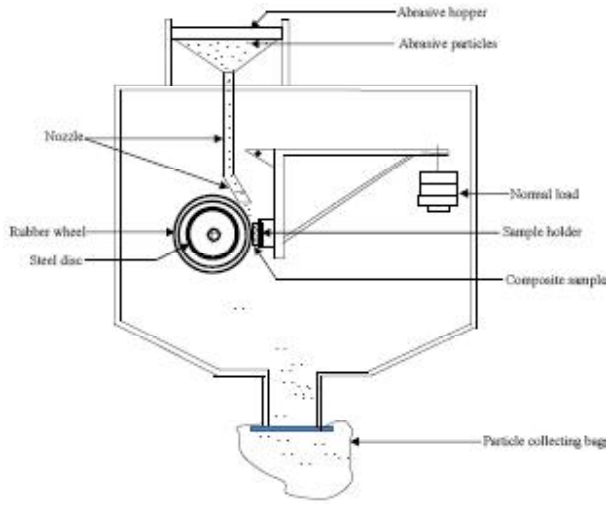


**Figure 1 : Schematic diagram of abrasive jet machine**


**Figure 2 : SEM Micrograph of the used erodent**

**TABLE 1: Theoretical and measured density values of the composites with volume fraction of voids**

| Composites | Measured density (gm/cc) | Theoretical density (gm/cc) | Volume fraction of voids (%) |
|---|---|---|---|
| RGF+ Epoxy | 1.530 | 1.544 | 0.906 |
| RGF+ Epoxy+$Al_2O_3$ | 1.627 | 1.717 | 5.241 |
| RGF+ Epoxy+ pine bark dust | 1.650 | 1.705 | 3.225 |
| RGF+ Epoxy +SiC | 1.620 | 1.702 | 4.817 |

study is shown in figure 2. The abrasive was fed at the contacting face between the rotating rubber wheel and the test sample. The tests were conducted at a rotational speed of 100 rpm. The rate of feeding the abrasive was 255±5 g/min. The sample was cleaned with acetone and then dried. Its initial weight was determined in a high precision digital balance (0.1mg accuracy) before it was mounted in the sample holder. The abrasives were introduced between the test specimen and rotating abrasive wheel composed of chlorobutyl rubber tyre (hardness: Durometer-A 58-62). The diameter of the rubber wheel used is 228 mm. The test specimen was pressed against the rotating wheel at a specified force by means of lever arm while a controlled flow of abrasives abrades the test surface. The rotation of the abrasive wheel was such that its contacting face moves in the direction of sand flow. The pivot axis of the lever arm lies within a plane, which is approximately tangent to the rubber wheel surface and normal to the horizontal diameter along which the load is applied. At the end of a set test duration, the specimen was removed, thoroughly cleaned and again weighed (final weight). The difference in weight before and after abrasion was determined. At least three tests were performed and the average values so obtained were used in this study. The experiments were carried out for loads of 50N and 75N at a constant sliding velocity of 1.193 m/s. Further the abrading distances were varied in steps of 100 m from 100 to 600 m. For the second longer duration test; say 200 m distance, the abrasion tests were carried out on the very same wear track where first (i.e., 100 m) shorter runs were involved. The wear was measured by the loss in weight, which was then converted into specific wear rate using the measured density data. The specific wear rate ($W_S$) was calculated from the equation:

$$W_S = \Delta m/\rho t\, V_S.F_N \quad (5)$$

Where, $\Delta m$ is the mass loss in the test duration (gm), $\rho$ is the density of the composite (gm/mm$^3$), t is the test duration (sec), $V_s$ is the sliding velocity (m/sec), $F_N$ is the average normal load (N).

The specific wear rate is defined as the volume loss of the specimen per unit sliding distance per unit applied normal load.

## 3. RESULTS AND DISCUSSION

### 3.1. Density

The theoretical and measured densities along with the corresponding volume fraction of voids are presented in TABLE 1. It may be noted that the composite density values calculated theoretically from weight fractions using Eq. (3) are not in agreement with the experimentally determined values. The difference is a measure of voids and pores present in the composites. It is clear from the TABLE 1 that in A the volume fraction of

TABLE 2: Mechanical and physical properties of the composites

| Composites | Tensile strength (MPa) | Tensile modulus (GPa) | Flexural strength(MPa) | ILSS (MPa) | Impact energy(J) | Micro-Hardness(Hv) |
|---|---|---|---|---|---|---|
| RGF+ Epoxy | 249.6 | 6.70 | 368 | 18.42 | 1.561 | 34 |
| RGF+ Epoxy+$Al_2O_3$ | 204.5 | 5.92 | 351.84 | 22.57 | 1.704 | 38 |
| RGF+ Epoxy+ pine bark dust | 140.8 | 3.35 | 222 | 23.46 | 0.827 | 27 |
| RGF+ Epoxy +SiC | 179.4 | 6.07 | 297.82 | 18.99 | 1.84 | 42 |

voids is negligible and this is due to the absence of particulate fillers. With the addition of filler materials more voids are found in the composites. As the filler content changes from composites to composites the volume fraction of voids is also found to be changes. Density of a composite depends on the relative proportion of matrix and reinforcing materials and this is one of the most important factors determining the properties of the composites. The void content is the cause for the difference between the values of true density and the theoretically calculated one. The voids significantly affect some of the mechanical properties and even the performance of composites in the place of use. Higher void contents usually mean lower fatigue resistance, greater susceptibility to water penetration and weathering. The knowledge of void content is desirable for estimation of the quality of the composites. It is understandable that a good composite should have fewer voids. However, presence of void is unavoidable in composite making particularly through hand-lay-up route.

### 3.2. Tensile properties

The test results for tensile strengths and moduli are shown in TABLE 2 respectively. It is seen that in all the samples irrespective of the filler material the tensile strength of the composite decreases with the change in filler content of the composites. The unfilled glass epoxy composite has a strength of 249.6 MPa in tension and it may be seen from Table 2 that this value drops to 249.6 MPa and 140.8 MPa with addition of different filler materials with same wt percentage of filler contents. Among the three fillers taken in this study, the inclusion of pine bark causes maximum reduction in the composite strength. There can be two reasons for this decline in the strength properties of these particulate filled composites compared to the unfilled one. One possibility is that the chemical reaction at the interface between the filler particles and the matrix may be too weak to transfer the tensile stress; the other is that the corner points of the irregular shaped particulates result in stress concentration in the polyester matrix. These two factors are responsible for reducing the tensile strengths of the composites so significantly. Similar property modification has been previously reported for $Al_2O_3$ particles reinforced in polyurethane matrix.

The compatibility of SiC particles in epoxy resin seems to be not as good as that of $Al_2O_3$, as a result of which the percentage reduction in tensile strength is highest in the former case. The tensile modulus of these alumina filled composites is also found to be less than the modulus of the unfilled one. On the contrary the experimental findings suggest that with addition of SiC particle the tensile moduli of the glass epoxy composites improve reasonably.

### 3.3. Flexural and Inter-laminar shear strength

TABLE 2 shows the comparison of flexural strengths of the composites obtained experimentally from the 3-point bend tests. It is interesting to note that composites with addition of small amount (10 wt %) of alumina and SiC exhibited similar flexural strength compared to the unfilled glass-epoxy composite. But for the composite samples pine bark filled glass fiber epoxy composite with 10 wt% of these fillers lower values of the flexural strength are recorded.

The inter-laminar shear strength values of the particulate filled composites are shown along with that of the unfilled glass epoxy composite in TABLE 2. It is seen that there is no dramatically improvement of ILSS of glass-reinforced epoxy composites with particulate filling irrespective of the filler type. Incorporation of $Al_2O_3$ is seen to have caused the maximum increase in the strength compared to the other fillers.

### 3.4. Impact strength

The impact energy values of different composites recorded during the impact tests are given in TABLE 2. It shows that the resistance to impact loading of glass-epoxy composites improves with addition of particulate fillers. It is seen that with incorporation of $Al_2O_3$

Full Paper

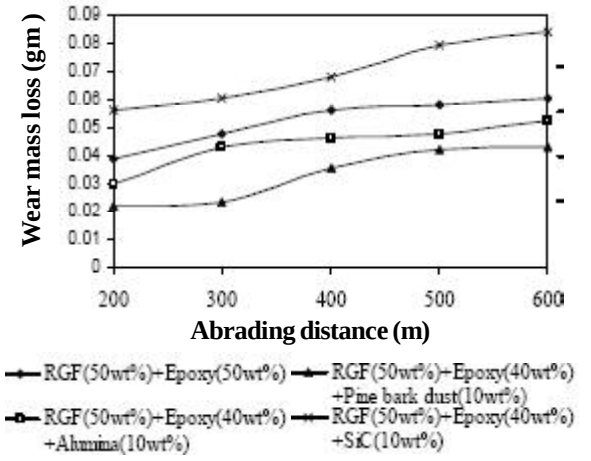


**Figure 3 : Wear volume of composites as a function of abrading distance at 50N for 300μm**

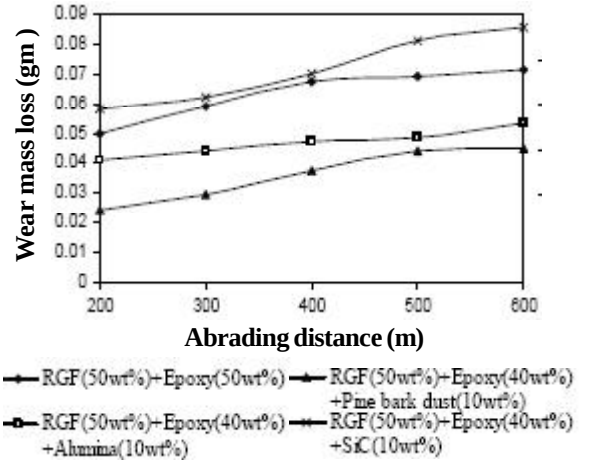


**Figure 4 : Wear volume of composites as a function of abrading distance at 75N for 300μm**

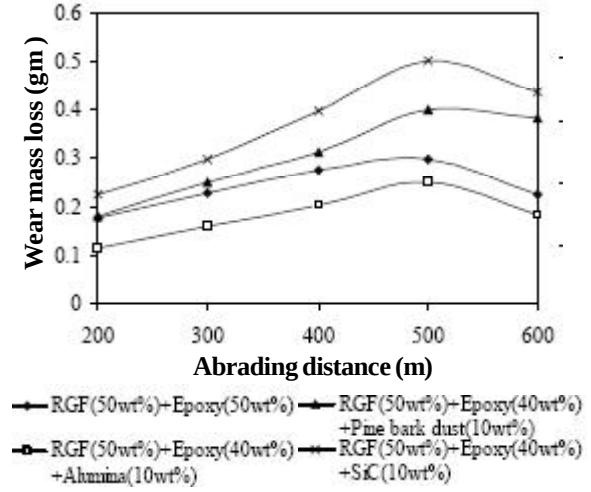


**Figure 5 : Wear volume of composites as a function of abrading distance at 75N for 400μm**

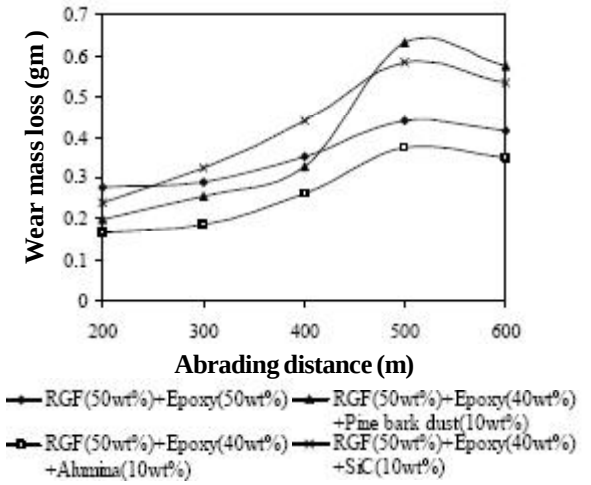


**Figure 6: Wear volume of composites as a function of abrading distance at 75N for 400μm**

and SiC particles the impact strength of unfilled glass fiber-epoxy composite increases by about 15% - 20% . It is also noteworthy that the $Al_2O_3$ filled composites show 10% - 15% higher impact strength compared to the unfilled one.

### 3.5. Hardness

The hardness of all the filled composites show similar values as compares to that of the unfilled composites (TABLE 2).

### 3.6. Abrasive mass loss and specific wear rate

Figures 3 and 4 show the wear loss in mass of the samples at 50 and 75N loads and 300μm abrading particle size, respectively. It is clear from these figures that for all the polymer composites used in this study there is a near linear wear mass loss with abrading distance. It indicates a steady-state wear with a constant wear rate. The highest wear mass loss is for filled SiC-RGF-Epoxy composite and the lowest is for Pine bark dust-filled RGF-Epoxy composites. In these figures for Alumina filled RGF-Epoxy and unfilled RGF-Epoxy composites there is an average increase in abrasion resistance.

Figures 5 and 6 show the abrasive wear mass loss of the composite samples at 50 and 75N loads and 400μm abrading particle size, respectively. It is clear from these figures that there is a near linear wear mass loss with abrading distance. The composites exhibited relatively high initial wear rates, when surfaces are new, which decreased gradually with increase in abrading

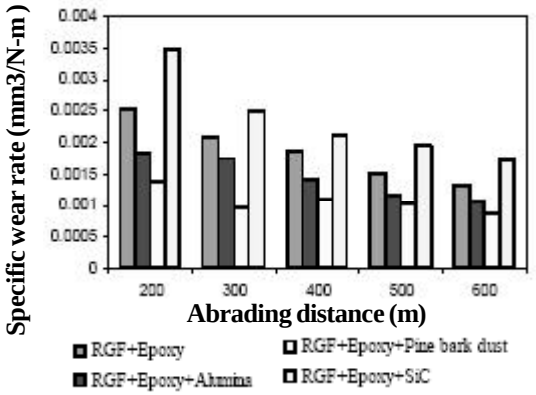


**Figure 7 : Specific wear rate of composites as a function of abrading distance at 50N**

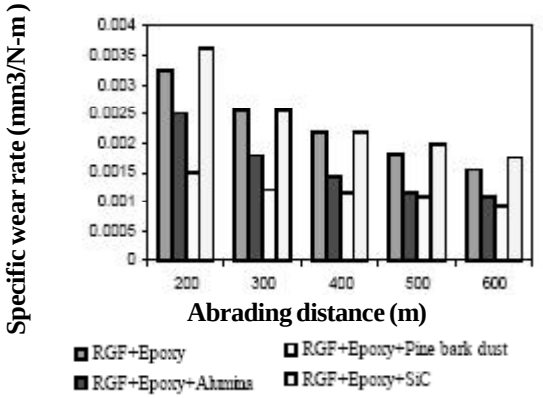


**Figure 8 : Specific wear rate of composites as a function of abrading distance at 75N**

distance. This is due to asperities and in homogeneity being rapidly worn until a uniform smooth surface is produced. The wear mass loss of composites at 50N load and 400μm erodent size lies in the range (0.177-0.3)gm for RGF-Epoxy, (0.113-0.2495)gm for RGF-Epoxy-Alumina, (0.18-0.402)gm for RGF-Epoxy-pine bark dust and (0.2234-0.5041) gm for RGF-Epoxy-SiC composites for 200 to 600m abrading distance as shown in figure 5, respectively. Also, from figure 6 the wear mass loss at 75N load and 400μm abrading particle size show similar mass loss patens observed (Figure 5) with increase in abrading distance. These results clearly indicate that the rate of wear mass loss increases with increase in abrading distances from 200m to 500m, but beyond 500m there is slight variation is observed (figures 5 and 6). This may be due to with the increase in abrading distance above 500m the matrix bonding strength between fiber, filler material and the matrix phase may be increased.

Figures 7 and 8 show the variation of specific wear rate in RGF-Epoxy, RGF-Epoxy-Alumina, RGF-Epoxy-Pine bark dust and RGF-Epoxy-SiC composites. At all abrading distances, the lowest specific wear rate is for pine bard dust filled RGF-Epoxy composites with a value of 0.000881 $mm^3$/(N-m) and the highest value at 0.003482 $mm^3$/N-m for SiC-filled RGF-Epoxy composites (Figure 7). For all composites of this study, the specific wear rate drops with increase in abrading distance. The specific wear rate for SiC-filled composites varies between 0.001722 and 0.003482 $mm^3$/(N-m) and for pine bark dust filled composites the value varies between 0.000881 and 0.001365 $mm^3$/(N-m) as shown in figure 7. Similar observation is also observed in Figure 6 with increase in load from 50N to 75N. The influence of fibers and/or fillers on the abrasive wear resistance of neat polymer is more complex and unpredictable and mixed trends are reported[11,12]. Lancaster[11] studied 13 polymers reinforced with 30% short carbon fiber and reported that reinforcement enhanced the wear performance of seven composites and that of six composites deteriorated. Sole and Ball[12] studied the effect of mineral fillers such as talc, CaCO3, BaSO4, and fly ash on abrasive wear of resistance of polypropylene (PP). They reported that the addition of mineral fillers to the PP matrix decreases the wear resistance under severe abrasion conditions. However, under mild abrasion conditions the shape and size of the reinforcing filler influences the wear performance. Thus in the present work also, similar observations were found which are in agreement with the findings reported in the literature[11,12].

### 3.7. Surface morphology

To correlate the wear data better, SEM photographs presented in figures 9(a and b) to pertaining to a load of 50 N and at different abrading distances for RGF-Epoxy, RGF-Epoxy-$Al_2O_3$, RGF-Epoxy-SiC and RGF-Epoxy-Pine bark composites are considered. figure 9(a) shows the abrasive wear surfaces of unfilled RGF-Epoxy composite at a load of 50N, 200m abrading distance and 9(b) shows the abrasive wear surface of unfilled RGF-Epoxy composites of load 50N, 600m abrading distance, respectively. The deep furrows in the abrading direction due to the ploughing action by sharp abrasive particles are seen on the surface. At higher

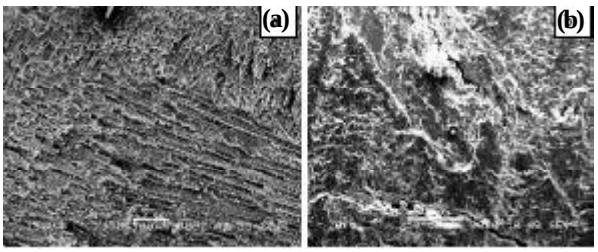


**Figure 9: Photomicrographs of worn surface of RGF-epoxy composites: (a) 200 m, 50 N and (b) 600 m, 50N**

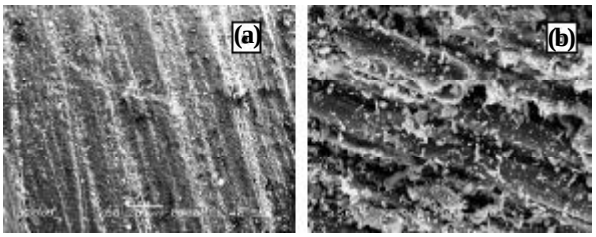


**Figure 10: Photomicrographs of worn surface of pine bark dust-RGF-Epoxy composites: (a) 200 m, 50N and (b) 600 m, 50N**

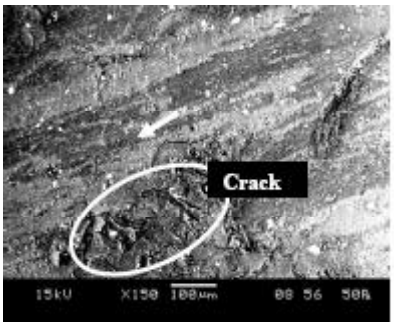


**Figure 11: Plastic flow of matrix material in the sliding direction: SiC-RGF-Epoxy composites at 200 m abrading distance and 50N load**

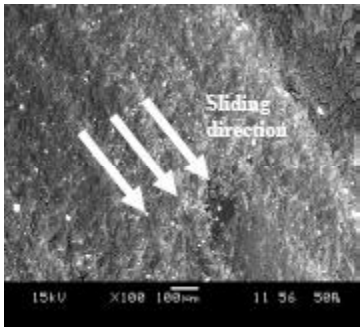


**Figure 12 : Formation and propagation of cracks at the fiber-matrix interface: Alumina-RGF-Epoxy composite at 300m abrading distance and 50N load**

abrading distance, photomicrograph shown in figure 9(b) depicts severe damage to the matrix, more fiber breakage and some fibers are pulled-out from the surface. In this figure the brittle fracture of the material due to the cutting action by the abrasive particles are apparent and the extent of damage to the matrix and fiber is severe compared to lower abrading distance (**Figure** 9(a)).

Photomicrographs, Figures 10(a and b) record the pattern of abrasion wear in pine bark dust filled random glass fiber epoxy composites. The pine bark dust filled composites system shows less of matrix phase wear out in figure 10(a). The protrusion of the phase and resultant less wear out are seen in figure 10(b). In pine bark dust filled composite the samples, as it contains a combination of hard and soft phases, severity and extent of damage on the specimen surface becomes less, in the softer regions as noticed owing to the presence of hard pine bark dust particles. As the hard phases/regions offer resistance to the damaging action of the abrasive, less of the damage is noticed in these systems. The SEM pictures amply demonstrate greater occurrence of debris that includes broken fibers when system is subjected to wear. Thus this observation lends credence to the contention that the presence of pine barks dust particles allow less of matrix wear during abrasion which in turn leads to lower fiber breakage.

From **figure** 11 the material is removed from the sample mostly by the adhesion mode. It can be seen that there is a plastic flow of the matrix material in the abrading direction which is indicated by the arrow. It is understandable that as the sliding proceeds, the resin soften due to frictional heat generation. As a result, the SiC particles and the glass fiber easily tear the matrix and gradually get aligned along the abrading direction. These particles by virtue of their size, shape, brittleness and high hardness influence and modify the wear behavior of the composites. Further, crack formation and propagation can be seen figure 12 at the matrix fiber interface, which also contribute to material loss over the test duration.

## 4. CONCLUSIONS

Based on the analysis of experimental results and findings the following conclusions can be drawn: This work shows that successful fabrication of a multi component hybrid composite (using epoxy as matrix, random glass fiber as reinforcement and alumina, SiC and

pine bark dust as filler) is possible by simple hand lay-up technique. An environmental waste like pine barks dust as a filler material can also be gainfully utilized for the composite making purpose. Incorporation of these fillers modifies the tensile, flexural, and impact strengths of the composites. A steady decline in the tensile strength is noticed in the filled composites whereas the presence of these particulate matters has caused improvement in impact strengths of the composites. The micro-hardness, density and flexural properties of the composites are also greatly influenced by the type and content of fillers. Abrasive wear rate decreases with increase in abrading distance for all the samples. However, the pine bark-filled composite showed better abrasive wear resistance. Abrasive wear rate is higher in SiC-filled glass fiber-reinforced epoxy composites.

## REFERENCES


**[1]** K.H.Zum Gahr; Tribol.Int., **31**, 587 **(1998)**.

**[2]** A.P.Harsha, U.S.Tewari; Polym.Test., **22**, 403 **(2003)**.

**[3]** M.Cirino, R.B.Pipes, K.Friedrich; J.Mater.Sci., **22**, 2481 **(1987)**.

**[4]** M.Cirino, K.Friedrich, R.B.Pipes, Composites, **19**, 383 **(1988)**.

**[5]** C.Lhymn, K.E.Tempelmeyer, P.K.Davis; Composites, **16**, 127 **(1985)**.

**[6]** H.Voss, K.Friedrich; Wear, **116**, 1 **(1987)**.

**[7]** B.J.Briscoe, L.H.Yao, T.A.Sto¨larski; Wear, **108**, 357 **(1986)**.

**[8]** A.P.Harsha, U.S.Tewari; Polym.Test., **21**, 697 **(2002)**.

**[9]** A.P.Harsha, U.S.Tewari; J.Reinf.Plast.Comp., (in press).

**[10]** B.D.Agarwal, L.J.Broutman; 'Analysis and performance of fiber composites', 2nd Edition, John Wiley and Sons; Inc., **(1990)**.

**[11]** J.K.Lancaster, A.D.Jenkins; Friction and Wear Polymer Science: A Material Science Hand Book.North Holland, Amsterdam, 959 **(1972)**.

**[12]** B.M.Sole, A.Ball; Tribol.Int., **29**, 457 **(1996)**.